UDC 669.18-412: 621746.6

PHYSICAL MODELING OF BILLET RHOMBOIDITY PHENOMENA DURING SOLIDIFICATION IN THE CCM MOULD

O. Smirnov, V. Ukhin, Y. Smirnov

Donetsk National Technical University

Abstract

Considerable efforts have been made in academic studies and industry toward higher casting speed in order to improve productivity in the continuous casting. The existing approaches to high-speed continuous billet casting are considered. The matter of present paper will be focused on the comparative analysis of heat removal intensity influence on the nature of solid shell formation in the mould. The solidifying shells are highly sensitive to a variety of distortion and crack problems. To investigate these problems, models have been developed to simulate coupled thermal and mechanical behavior of solidifying steel shell during continuous casting. Chemical substance Camphen ($C_{10}H_{16}$) was used as a model substance, the material is known for its dendrite microstructure during solidification. Physical modeling results of solid shell formation in the mould are presented and major factors affecting shell growth rate are determined. This article presents a mechanism for the formation of billet rhomboidity phenomenon based on a careful analysis of extensive measurements on physical optical model.

Keywords: continuous casting, billet, mould, solid shell, solidification, cracks, rhomboidity

Introduction

Continuous casting technology development has received much attention from researchers and producers during the past several decades, owing to the pursuit of maximum increase in casting speed and obtaining high quality products – fit with geometry requirements and free form surface and subsurface defects [1, 2]. Reported advance in billet continuous casting is often associated with the application of a tubular mould, the inner chamber of which is known to be of complex geometry. This geometry, to a large degree, accounts for the character of solidifying shell growth in the mould (i.e. heat removal, solidifying shell growth rate around the perimeter, shell shrinkage, internal stress in a solid shell, etc.) [3-5].

A quasi-parabolic profile in its bottom part is a distinctive feature of a tubular mould designed for specific process requirements (casting speed, steel composition, etc.). Though, commercial operating conditions of tubular moulds do not reveal full compliance of parabolic profile and optimal casting conditions. Moreover, field operation results in local wear of tubular mould surface (mostly at corner regions of a tubular mould bottom part), which in its turn deteriorates heat removal from billet surface and contributes to solid shell buckling. It is assumed that the profile of a tubular mould upper part is not of minor importance. As a matter of fact, to ensure high casting performance we must consider these conceptual framework during casting, and more importantly, in case of process variables deviation from the rated ones.

Major disturbing contributors influencing the formation of solid shell are adopted in this work; these are heat removal distribution down billet faces and corner regions, as well as inhomogeneous heat removal related to local wear of some inner mould surface either with shell detaching and associated air gap formation between the strand surface and inner tubular mould surface due to discrepancies in their contours.

Physical Modeling

Physical modeling technique is supposed the most efficient method for investigating the solidifying dynamics in different cast products, since this method allows for heat removal control from the cast product in question and for visualization of processes associated with solid phase growth [6]. The choice of model substance has gained considerable importance whereas it must meet the requirement of optical transparency and support thermo-physical properties, which provide appropriate set of similarity criteria. The present authors assume that dendrite microstructure during this substance solidification is an additional yet crucial modulation criterion.

For this study, chemical substance Camphen (2,2-Dimethyl-3-methylenbicyclo[2.2.1]heptan, 3,3-Dimethyl-2-methylennorcamphan) was found to be the most suitable material for the modulation of the solidifying strand characteristics, while it satisfies the above-mentioned requirements to a considerable degree and is of dendrite microstructure during solidification. Camphen optical transparency in the liquid phase is preserved till its complete solidification, thus enabling the visualization of solidification front advance. Camphen thermo-physical parameters were measured in the laboratory environment and are summarized in Table 1.

Table 1. Physical and thermo-physical properties of Camphen

Solidus temperature (°C)	Liquidus temperature (°C)	Solidification heat (kJ/kg)	Heat capacity (kJ/(kg·K))		Thermal diffusivity (m^2/c)	Surface tension (H/m)	Kinematic viscosity (m^2/c)
			Liquid	Solid			
33	35	40,2	2,4	2,1	$1{,}3\cdot10^{-8}$	0,021	$7{,}2\cdot10^{-6}$

Basic schematics of laboratory apparatus are illustrated in Fig. 1. Liquid Camphen solidifies in the cross-section of model billet CCM mould made of aluminum alloy (Fig. 1, Pos. 1), which guarantees high intensity of heat removal.

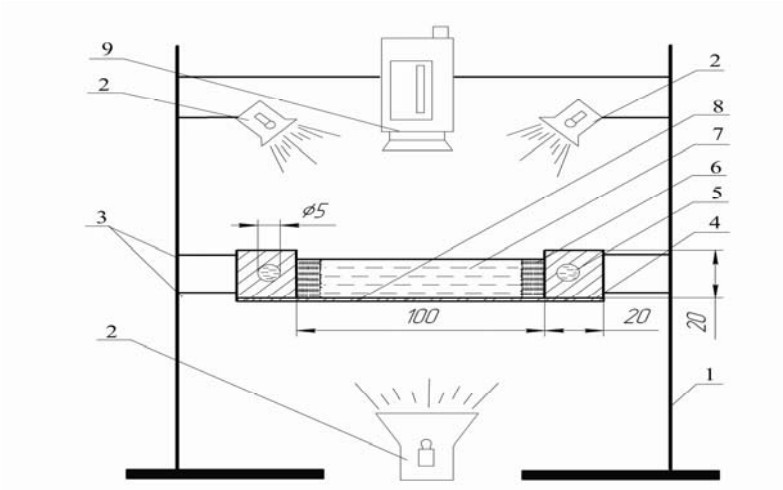

Figure 1 – Schematics of laboratory facility for the modulation of billet solidification in the mould: 1 – fixing frame; 2 – lighting equipment; 3 – mould holders; 4 – mould; 5 – jet openings for cooling water; 6 – Camphen solid layer produced due to solidification; 7 – model substance liquid layer; 8 – transparent acrylic resin of low thermal conductivity; 9 – video camera.

The model liquid depth was 20 mm. Copper tubes were mounted inside the model mould (Fig. 1, Pos. 2). Cooling water of appropriate flow rate passed through copper tubes of 5 mm in inner diameter. The model bottom part is equipped with a transparent plexiglas (Fig. 1, Pos. 3), which allows us to observe solidification processes while transmitting light through liquid substance bath. Accordingly, the proposed scheme results in increase of heat removal intensity through water-cooled model walls: it becomes significantly higher than that through modeling substance meniscus and transparent plexiglas. The physical model is made with geometrical scale factor 1:1 with respect to its industrial counterpart – concast billet of 100x100 mm in cross-section. Camphen pouring temperature averaged 42 ± 0.5°C. Water temperature for walls cooling was about 18-20°C. Solidification process was observed and recorded with a digital video camera. The investigation of solidification and crack formation kinetics in a solidified steel shell was carried out by quantitative assessment of data obtained from video files.

The developed model provides for adjustments of water flow-rate separately for every face and for flow-rate measurements with flow meter. Water temperature to within ± 0.1°C was gauged with mercury thermometer at inlet and outlet of the model. An air gap between the model mould and solidifying steel shell was modulated by means of sticking of heat insulation gasket (of estimated thickness) on the inner mould wall or corner area.

The differences in the thermo-physical characteristics of steel and Camphen were compensated by adjusting the heat removal intensity modes so as to fit the similarity parameter of the product of Bio (Bi) criterion and phase transition (N) criterion (Bi · N = idem). Modeling time scale μ_τ was determined on the basis of Fourier identity criterion (Fo = idem). Moreover, effective values of thermal diffusivity in the developed two-phase region were defined with the following Equation:

$$a_{эф} = \lambda / \rho\left(C + L / \Delta T_{кр}\right)$$

where λ is the thermal conductivity of the substance (W/(m·K)); ρ is the substance density (kg/m^3); C is the mass heat capacity (kJ/(kg·K); L is the substance solidification heat (kJ/kg); $\Delta T_{кр}$ is the range of solidification temperatures (°C).

The following established experimental squared relationship was used for comparative quantitative assessment of solidified shell growth dynamics against cooling conditions:

$$\delta = k \times \sqrt{\tau}$$

where δ is the solid shell thickness; τ is the solidification time; k is the experimentally measured solidification factor.

The dynamics of solidification process is readily predicted by the value of solidification factor *k*, since the solid shell thickness for specified solidification time is determined in the course of physical modeling.

Results and Discussion

The first investigation phase included estimation of the cooling intensity influence on the solid shell growth. For this reason, two associated mould faces were water-cooled, water flow-rate being 0.818 l/min per each face. Two other faces were cooled with water flow-rates of 0.409 l/min and 0.080 l/min respectively. The experiment results are presented in Fig. 2.

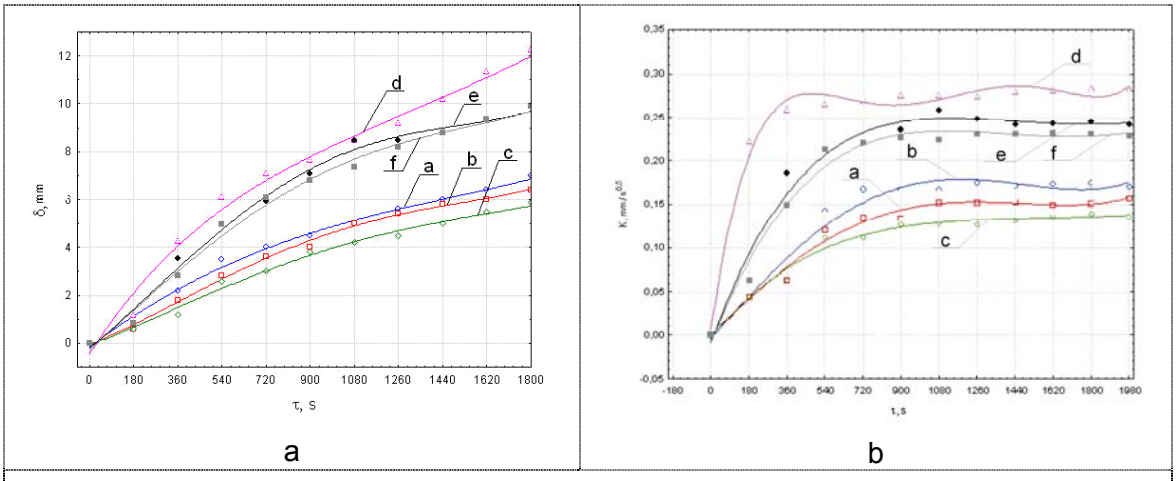

Figure 2 – Dynamics of solidification front advance a and the dependence of solidification factor b on the model faces cooling mode: a,d – cooling intensity 0.818 l/min; b,e – cooling intensity 0.409 l/min; c,f – cooling intensity 0.080 l/min.

When analyzing the obtained results two solidification stages of the studied samples were distinguished. The first stage (initial solidification) involves continuous increase in the value of solidification factor *k* till it equals the specified magnitude dependent on heat removal intensity.

Afterwards, the value of solidification factor *k* remains constant for a long time interval. This last factor seems to indicate that the solid shell growth exhibits high stability degree in the first solidification stage. Therefore, it was the first solidification stage when the comparative analysis of solid shell formation dynamics was carried out.

Through consideration of experimental data, it was shown that the 50% decrease in flow-rate of water for model walls cooling leads to 6.0-6.5% decrease in the model solid shell thickness in the face centre and to 14.0-14.5% decrease in the solidification factor value.

The above-mentioned decrease in water flow-rate brought different results for model corner regions: solid shell thickness was 17.5-18.0% reduced, while solidification factor value was 21.0-21.5% reduced. Further decrease in water flow-rate to 0.08 l/min have led to 14.0-15.0% and 17.0-18.0% decrease in solid shell thickness, and 18.0-19.0% and 19.0-20.0% decrease in the solidification factor value. Hence, change of heat removal conditions for a given physical model is related to adequate change in solid shell growth rate. Furthermore, nonuniform solid shell thickness around the billet perimeter causes the internal tensile and compression stress development, which turned out to produce cracks in the solid phase.

Having in mind that solid shell detaching from the inner tubular mould surface (due to the profile distortion or wearing of surface tubular mould areas) can be observed in continuous casting practice, the second investigation phase comprised experiments aimed at the elucidation of air gap effect on the strand solidification dynamics and on the crack origination in the shell. However, two most expected conditions were considered: air gap formation at the mould corner regions and air gap formation along the mould face.

To modulate the decrease in heat removal intensity during the solid shell detaching from the model mould corner (or face centre), the sticking of appropriate heat insulation gasket was applied. In the course of testings, the heat insulation layer thickness was varied (1.0 and 2.0 mm), thus providing for heat removal intensity change. It was concluded that the decrease in heat removal intensity is readily evident at the onset of solid shell formation (shell thickness of up to 6.0-8.0 mm). While modulating the heat removal intensity reduction at the billet corner region, the substantial (up to 5.0-6.0 mm) lagging in solidification front advance in the presence of heat insulation gaskets was registered. Afterwards, we observed reasonable stability in the solid shell growth rate, which is corroborated by close values of solidification factor *k*. Meanwhile, the photographs presented in Fig. 3 demonstrate that the attribute of solid shell formation in the regions of reduced heat removal (heat insulation gaskets applied) is the origination of numerous shallow cracks, which are arranged along heat removal direction.

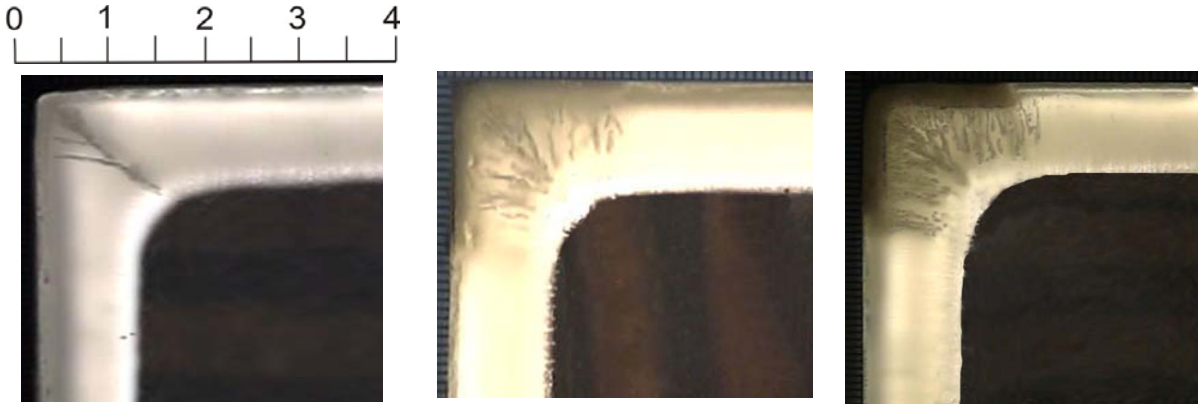

a b c

Figure 3 – Typical solid shell after strand solidification in the mould: a – in the absence of heat insulation; b and c – in the presence of 1mm and 2 mm heat insulation located in the mould corner region

Shallow cracks distribution is seen of local character, they are arranged around the placing area of heat insulation gaskets perimeter. The cracks are found to be thin breakouts of solid shell continuity extending along the dendrite crystals boundaries at 5.0-8.0 mm depth. One of the main conclusions is that the cracks quantity per unit of solid shell perimeter length increases with the rise in heat insulation gasket thickness.

We consider this phenomenon as related to the proposed mechanism of crack formation: crack formation is exerted by the internal stress in the solid shell, which is produced by inhomogeneous shell cooling. Crack formation was observed in solid shell regions with the following features: weakly cooling and minor value of linear shrinkage as contrasted to the solid shell regions of higher solidification rate.

The proposed mechanism of crack formation in the solid shell under local heat removal decrease was further investigated by heat insulation gaskets placing along the model faces. Fig. 4 reflects typical modeling results: heat insulation gasket was placed along the horizontal (position in photograph) face, while the vertical face was free of insulation. Solid shell thickness of 4.5 mm and 6.0 mm (no heat insulation applied at cooling) was reduced in the face centre (heat insulation layer applied) in 2.25 and 1.4 times respectively. Moreover, the solidification front seems to advance with constant rate in every situation considered, this phenomenon is concerned with increase in thermal resistance to heat removal through solid shell.

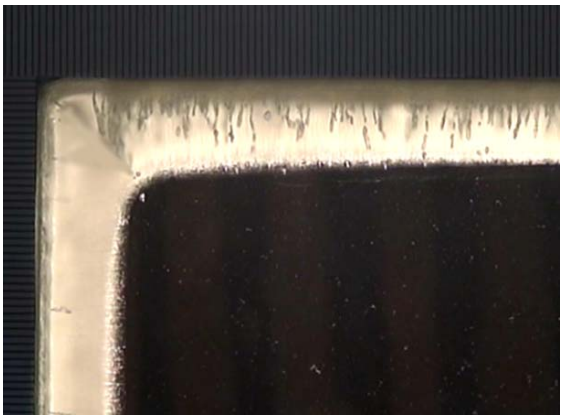

Figure 4 – Crack origination in the process of solid shell formation, heat insulation placed on the mould face

On the basis of experimental results, we arrived at conclusion that there is a clear dependence between change in local heat removal intensity from the solid steel shell in the CCM mould and formation of numerous shallow cracks arranged around the billet perimeter with special emphasis on the regions of weak heat removal intensity. Inhomogeneous steel shrinkage around the strand perimeter as well as low strength and plasticity of solid shell at solidification point [7] seem to account for crack formation in the solid shell. Cracks mostly appear in the regions of minor shrinkage due to the rise of tensile stress caused by intense shrinkage in the associated regions.

On adopting the proposed mechanism of solid shell formation in the CCM mould, it is suggested that in billet corner regions detached from the tubular mould surface, the origination of microcracks can occur, which weaken the solid structure. On the other hand, owing to internal stresses formed in the solid structure during solidification, billet corner regions (sensitive to crack formation) display a tendency to macrodistortion. As a consequence, strand cross-section geometry is being changed, giving rise to rhomboidity or another complex geometry. Additionally, Fig. 5 shows that in the billet corner regions, longitudinal macro- cracks can be formed, this indicates severe deterioration of the concast billet quality.

a b

Figure 4 – Typical arrangement of longitudinal cracks on billets transversal templates (125 mm squares): a – 18 mm rhomboidity; b – 16 mm.

Conclusions

1. The growth rate of the solid steel shell in the concast mould is found to be of inhomogeneous nature. At the initial solidification stage, solidification factor *k* value is observed to increase continuously; afterwards, its value turns out constant. Solid shell growth rate at corner regions 1.5-2 times exceeds the growth rate measured at off-corner regions; this attributes to two-dimensional heat removal pattern at the mould corner regions.

2. The decrease in heat removal intensity at any solid shell area leads to decrease in shell growth rate in the relevant area, this accounts for origination of numerous cracks in the solid structure, which eventually bring the local weakening of strand solid shell and can cause shell distortion (buckling).

3. Inhomogeneous growth rate of solid shell around the billet perimeter determines the internal stresses rise in the solid structure, which are ultimately responsible for the billets contour distortions and for producing typical geometry and surface defects, i.e. rhombic deformation and subsurface longitudinal off-corner cracks.

References:

1. Wolf M. Can mini mills cope with high speed casting? / M. Wolf // Steel Times International. – 1989. – №3. – P.16-19.
2. Liu Jian, Xu Maoqing, Sepp Kohl e.a. Operational success of a 5-strands high speed Convex Technology billet caster for SBQ steels at Shagang Steel, China // SEAISI Singapore Conference, 14-16 May, 2001. – Singapore: SEAISI, 2001. – 9 p.
3. Krujelskis V., Cook J. The Influence of Mold Taper and Distortion on Cast Billet Quality // Steelmaking Conference Proceedings (ISS). – 1988. Vol.71. – P.349-352.
4. Kittaka S., Uehara M., Sato T., Higashi H. High Speed Casting Mold for Billet Caster (NS Hyper Mold) // Nippon Steel Technical Repport. 2000. No.82 July. – P.65-70.
5. Park J.K., Li C., Thomas B., Samarasekera I.V. Analys of Thermo-Mechanical Behavior in Billet Casting / // Proceedings 60th Electric Furnace Conference. ISS. – Warrendale, PA, 2002. – P. 669-685.
6. Thomas B.G. Continuous casting: Complex Models // The Encyclopedia of Materials: Science and Technology. – Oxford: Elsevier Science Ltd. Vol.2. 2001. – pp.1599-1609.
7. Strategies for coupled analyses of thermal strain history during continuous solidification processes / J.R.Boehmer, G.Funk, M.Jordan, F.N.Fett // Advanced in Engineering Software. 1998. Vol.29. No.7-9. – P.679-697.

Received on 25.03.2011